Immediate and sustained effects of cobalt-containing pigments on macrophages

Julie Devcic[1]†, Bastien Dalzon[1]†, Manon Dussol[2], Véronique Collin-Faure[1], Julien Pérard[1], Daphna Fenel[3], Guy Schoehn[3], Marie Carrière[2], Thierry Rabilloud[1]*

1 Chemistry and Biology of Metals, Université Grenoble Alpes, CNRS UMR5249, CEA, IRIG-DIESE-LCBM-ProMIT, F-38054 Grenoble

2 Université Grenoble-Alpes, CEA, CNRS, IRIG-DIESE, SyMMES, Chemistry Interface Biology for the Environment, Health and Toxicology (CIBEST)38000 Grenoble, France

3 Institut de Biologie Structurale (IBS), University Grenoble Alpes, CEA, CNRS, Grenoble 38044, France

†: these authors contributed equally to this work

*: to whom correspondence should be sent: thierry.rabilloud@cnrs.fr

Abstract

Tattoos are trending, and in the USA 25% of people aged 18 to 50 are tattooed. The more people get tattoos, the more skin injuries are discovered and reported in the literature. The short-term and localized effects are well known, but injection of tattoo inks can be associated to long-term risks. In this article, we investigated three cobalt pigments, which constitute a wide range of colors found in tattoos: Pigment Violet 14 (purple), Pigment Green19 (green), and Pigment Blue 28 (blue). After injection, macrophages are among the first cells to come in contact with pigments. We thus tested the effects of cobalt-based pigments on the macrophage cell line J774A1. In order to detect delayed effects, we compared two exposure schemes: acute exposure for 24 hours and with a 3 days post-exposure recovery period. The conjunction of these two schemes allowed the investigation of delayed or sustained effects of the pigments. Pigment dissolution and cobalt release was very variable from one pigment to another, Pigment Violet 14 and Pigment Green19 being easily dissolved, while Pigment Blue 28 dissolved much more slowly. The cytotoxicity of the pigments correlated well with their dissolution. All pigments induced functional effects on macrophages, which were largely pigment-dependent. For example, Pigment Green19 and Pigment Blue 28 showed a delayed effect on the phagocytic capacity of the cells. All three pigments induced a low but significant secretion of tumor necrosis factor, but the effect was transient. Conversely, Pigment Violet 14 and Pigment Blue 28 induced a sustained secretion of interleukin 6, although at low levels. The pigments also induced changes in some important membrane markers of macrophages such as CD11b, PdL-1 or CD206. In conclusion, the pigments induced functional perturbations in macrophages, sometimes persistent over time after exposure, even at non-toxic doses.

1. Introduction

Tattooing is an ancient practice which originated in the Stone Age, 6000 years b.c.[1,2]. It consists in the intradermal injection of non-biodegradable and persistent inks and historically corresponds to specific medical, cultural, ritual or social roles. Tattoos are not limited to only black ink (carbon black), and the use of different inks, although increasing recently, traces back far in the past [3]. Thus, tattoos are generally based on a wide range of colored substances in suspension and these mixes of substances are not always known due to insufficient regulations [4]. These pigmentary materials can be composed various organic (e.g. azo) , organometallic (e.g. metal phthalocyanines) or mineral pigments [4]. Tattoos are trending and increasingly appeal to youngsters. In the USA, 25% of people aged 18 to 50, are tattooed. In Europe, the prevalence is approximately 10% [5]. Moreover, tattoos cover a larger surface and tend to be composed of more colors than before. These factors account for the rise in skin injuries such as dermatose or neoplasia reported in the literature [5,6]. These short-lived and localized effects (e.g. hypersensitivity skin reaction) are widely known [7] .However, the injection of tattoo inks can also be associated to long-term risks. Indeed, tattooing seems to be associated with several cases of skin cancer (e.g. melanoma or carcinoma) , which incidence appears to be color- or material-dependent. Red inks (composed of azo pigments), for example, increase UV-induced cancers[8]. Black and dark blue pigments used in tattoos seem to be linked to the majority of post-tattoo skin cancers. These inks may contain carcinogenic substances, e.g. present as impurities in carbon black [9], such as polycyclic aromatic hydrocarbons (PAHs) and phenols [10]. Certain inks contain monoazopigments (e.g. yellow or red inks) or heavy metals such as mercury sulfide (red), cadmium (from yellow to red), chromium oxide (green), and cobalt (from purple to green), which are also suspected carcinogens [9,11,12].

After intradermal injection, pigments are internalized by three main cells: fibroblasts, neutrophils, and macrophages. Neutrophils are mainly present at the site of injection immediately after the injection due to mechanical injuries comprising blood losses, superficial infections [13], inflammations, etc. caused by the penetration of the needle into the dermis. These short-lived cells (about 24h) are then quickly eliminated by macrophages via the efferocytosis process and are subsequently absent from the tattoo site in the long term. Fibroblasts internalize a low quantity of pigments contrary to macrophages which are professional phagocytic cells and ensure the lifelong persistence of tattoos inks in the dermis due to successive cycles of pigment capture, release and recapture. Indeed, dead macrophages are replaced by mostly new monocyte-derived macrophages or, to a lesser extent, via a local process of self-renewal [14,15].

In this article, we decided to assess the immediate and persistent effects of some pigments used in tattoo inks on macrophages because of their key role in the persistence of tattoos [14,15]. An impairment of their functionalities could induce damage to tissues and cause other diseases [16,17]. Furthermore, several articles showed that tattoo ink pigments can be found in lymph nodes due to both passive transport and active transport via macrophages [18]. This is especially true several weeks after the injection of tattoo ink when around 30% of the ink has been eliminated via blood or lymphatic circulation [19–21]. However, the presence of pigments-loaded macrophages in the lymph node can be due to migration of particles-loaded macrophages from the tattoo site to the draining lymph nodes, as suggested by some authors with other mineral particles [22,23]. Whatever the mechanism, massive absorption of pigments by macrophages might change their functions, and thus alter the immune homeostasis at the tattoo site and at distal sites such as the lymph nodes.

The present article investigates cobalt pigments, which constitute a wide range of colors found in tattoos (from purple to green) [24,25]. Although the exact nature of the pigments used in tatto inks is not disclosed, as it is considered as a trade secret, we chose to test three cobalt-based pigments referenced in the Colour Index International as PG19 (dark green), PB28 (blue), and PV14 (purple). Cobalt-based tattoo inks are authorized because the pigments themselves are authorized. However, cobalt is both an essential element (given that it is a cofactor of vitamin B12) and a toxic one at high doses [26]. It has shown deleterious effects on fibroblasts [27], leukocytes[28] and macrophages [29,30], and also a long-term

carcinogenic potential linked to slow cobalt release [31]. Thus, progressive cobalt release from pigments internalized by the macrophages may lead to alteration in their functions and phenotypes. This may represent a mechanism underlying potential long-term adverse effects of tattoos using these inks, therefore justifying this work. To this purpose, we used an in vitro murine macrophage system in a load-recovery mode, in which the cells are first loaded over 24 hours with the particles and then let evolve without added particles for three days [32,33].

2. Materials and methods

2.1. Pigment characterization

2.1.1.Pigment description

Pigment Blue 28 (Cobalt aluminate, $CoAl_2O_4$) and Pigment Violet 14 (cobalt phosphate) were purchased from Kama Pigments (Montreal, Canada). Pigment green 19 (mixed cobalt zinc oxide, deep cobalt green CO804) was purchased from Tokyo Pigment (Tokyo, Japan). Corundum (aluminium oxide spinel) was purchased from Sigma.
Pigments were received as powder. They were suspended in arabic gum (100 μg/ml) that had been previously sterilized overnight at 80°C, which was used as an anti-agglomeration reagent. The suspension was sterilized overnight again. Then, the suspension was sonicated in a Vibra cell VC 750 sonicator equipped with a Cup Horn probe (VWR, Fontenay sous Bois, France) with the following settings : time = 30min – 1 second ON, 1 second OFF – Amplitude = 60%, corresponding to 90W/pulse

2.1.2. Dynamic Light Scattering (DLS)

The pigments were diluted to 100 μg/ml with water or culture medium. Then, the size and dispersity of pigments were measured via Dynamics Light Scattering (DLS) using Wyatt Dynapro Nanostar instrument (Wyatt Technology, Santa Barbara, CA, USA).

2.1.3. Transmission Electronic Microscopy (TEM)

Negative Stain On Grid Technique (SOG): 10 μL were added to a glow discharge grid coated with a carbon supporting film for 3 minutes. The excess solution was soaked off using a filter paper and the grid was air-dried. The images were taken under low dose conditions (<10 e-/Å2) with defocus values comprised between 1.2 and 2.5 µm on a Tecnai 12 LaB6 electron microscope at 120 kV accelerating voltage using CCD Camera Gatan Orius 1000. The measurement was processed with Image J.

2.2. Cell culture and viability assay

The mouse macrophage cell line J774A1 was purchased from the European Cell Culture Collection (Salisbury, UK). For cell maintenance, Cells were cultured in DMEM containing 10% of FBS (fetal bovine serum) and 5μg/ml Ciprofloxacin. Cells were seeded every 2 days at 250 000 cells/ml and harvested at 1 million cells/ml.
For treatment with pigments, the following schemes of exposure were used:
i) An acute (24) exposure with pigments: Cells were seeded in 12-well adherent or non-adherent plate (according to the test) at 1 million cells/ml in DMEM containing horse serum 1% (HS 1%) and 5 μg/ml of Ciprofloxacin. Cells were exposed to pigments on the following day and analyzes at the end of 24h of exposure with pigments.

ii) A recovery exposure for 4 days: Cells were seeded in 12-well adherent plate at 1million cells/ml in DMEM supplemented with horse serum, as described above. After 24 hours of exposure to pigments, the medium was changed in order to remove pigments. The fresh medium was left for 48 more hours and changed again for 24 hours in culture before cells harvesting. The choice of a medium supplemented with low serum concentration was made to

limit cell proliferation during the recovery period (Dalzon et al. unpublished results). Cell proliferation during recovery has been observed previously [32], and is not likely to reflect the in vivo situation.
After exposing the cells to various concentrations of pigments, the viability of the cells was tested. Cells were flushed and harvested with PBS and centrifuged 200 g for 5 min. Pellets were resuspended in PBS with propidium iodide (PI) at a final concentration of 1 μg/ml. The percentage of viability was measured via a FacsCalibur flow cytometer equipped with the CellQuest software program (6.0, Becton Dickinson Biosciences, Le Pont-de-Claix, France) and settings corresponding to PI (480nm excitation and 600 nm emission). For every pigment tested, the LD20 was determined.

2.3. ICP-AES: Pigments Dissolution

2.3.1. In vitro dissolution

Pigments at just below the LD20 concentration: 2.5μg/ml and 500μg/ml were mineralized in aqua regia (1:3 mixture of nitric acid and hydrochloric acid, optimally in a molar ratio of 1:3). Samples were diluted in 10% nitric acid prior to analysis by inductively coupled plasma atomic emission spectroscopy (ICP-AES) on a Shimadzu ICP 9000 with Mini plasma Torch instrument, used in axial reading mode. A standard range of cobalt, zinc and aluminium (from 3.9 μg/L to 10 mg/L) was prepared for quantification.

2.3.2. In vivo dissolution

Cells were seeded in 6 wells plate at 1 million cells/ml in DMEM containing 1% horse serum and 5μg/ml Ciprofloxacin. They were exposed to nanoparticles on the following day, For recovery exposure, the pigment-containing medium was removed, replaced by fresh medium and left for 48 more hours. The culture medium was changed one more time and cells were left for 24 hours in culture. After 24h (acute exposure) and 96h (recovery exposure), the medium was removed and the cells rinsed with PBS. The cells were then lysed with 600 μl of lysis buffer (HEPES 5mM, spermine tetrahydrochloride 0.75 mM, SB 3-14 0.1%). 50μl of the crude lysate was collected and total protein was quantified with a modified dye-binding assay [34]. The remaining lysate was centrifuged at 10 000 g for 10 minutes to sediment the nuclei and the undissolved pigments, and the supernatant collected. Samples were kept at -20°C until mineralization.

The samples were thawed and mineralized by the addition of one volume of suprapure 65% HNO_3 and incubation on a rotating wheel at room temperature for 18 h. The samples were then diluted up to 6 ml with 10% nitric acid and the metal concentrations measured as described above. The results were normalized by the protein concentration in the samples, used as an indicator for cell number.

2.4. Internalization ability

2.4.1. Phagocytic activity measurement

The phagocytic activity was measured as previously described [35,36] using fluorescent latex beads (solid = 2,5%, 1μm diameter fluorescent yellow-green, catalog number L4655 from Sigma). The green fluorescence internalized by cells allows to quantify the phagocytic activity. The cell culture was performed as described previously. Cells were seeded into 12 well plates and exposed to pigments (Acute or recovery exposure) at 37°C, 5% CO_2. For the preparation of beads, the fluorescent beads were coated in a mix of horse serum and PBS (50% each by volume) for 30 min at 37°C (2,2μL of fluorescent latex beads for 1ml of mix). One hundred microliters of this solution were added per ml of cell culture, and the cells were

incubated for 3 hours at 37°C. Cells were harvested and washed with PBS, centrifuged 5 min at 1200 rpm; the pellets were suspended with 400 μl in PBS – propidium iodide 1 μg/ml, and analyzed by flow cytometry.

2.4.2. Neutral red assay

This molecule stain dyes lysosomes via active transport, and is thus a good indirect assay for lysosomal function. Cells were seeded in adherent 12-well plates and exposed to pigments (Acute or recovery exposure) at 37°C, 5% CO_2. 2 mg/ml neutral red in EtOH 50% was prepared and 10μl of this solution was added to every well containing 1 ml of culture medium and incubated for 2 hours at 37°C. After incubation, cells were washed twice with PBS and eluted with 2 ml of acid-alcohol solution (acetic acid 1% v/v, ethanol 50% v/v). The plates were incubated for 30 min at room temperature on a rotating table. The red color released was read at 540 nm [37]. To normalize the results, the number of adherent cells was estimated via a crystal violet assay. The fixed cell layer was rinsed twice with PBS and stained with crystal violet (4 μg/ml in PBS) for 30 minutes. Then, the cell layer was rinsed twice with PBS before elution with 1 ml of acid-alcohol solution. The purple color released was read at 590 nm using a spectrophotometer. The 540nm/590nm absorbance ratio was used as an index for the lysosomal functionality of the cells.

2.5. Inflammatory capacity assay

2.5.1. Nitric oxide (NO) production

The cells were grown to confluence in 12-well plates (harvested at 1 million cells/ml). Half of the wells were treated with 200 ng/ml LPS, and arginine monohydrochloride was added to all the wells (5 nM final concentration) to give a high concentration of substrate for NO synthase. After 18 hours of incubation, cell culture medium was recovered, centrifuged at 15,000 g for 15 min to remove pigments, non-adherent cells and debris. 500 μL of supernatant were collected. After the addition of an equal volume of Griess reagent, the mixture was incubated at room temperature for 20 min in order to wait for the completion of the reaction. The absorbance was read at 540 nm. To normalize the results, the number of cells in the culture plate was estimated by a crystal violet assay. The cell layer was rinsed twice with PBS and fixed with an acid-alcohol solution (acetic acid 1 % v/v, ethanol 50 % v/v) for 30 minutes. The cell layers were then stained by crystal violet as described in section 2.4.2.

2.5.2. Cytokine measurement

Tumor necrosis factor (TNFα), interleukin 6 (IL-6), were measured in the supernatant from cultured cells exposed to pigments and/or activated by LPS 200ng/ml, using the Mouse Inflammation Cytometric Bead Array kit (BD cytometric bead array, BD Biosciences, Rungis, France) according to the manufacturer's instructions. Measurements were performed on a Facscalibur flow cytometer, and the concentrations of cytokines secreted were assessed using FCAP Array Software.

2.6. Numerical Analysis

A Student's *t*-test was applied to all the results. Data are presented as means +/- standard deviations; * $p<0.05$,** $p<0.01$, *** $p<0.001$. Note that the systematic use of viability marker (propidium iodide or Sytox red) allows for analysis of live cells only. Biological experiments were driven on four independent biological replicates.

2.7. Comet assay

The presence of strand breaks in the DNA of cells exposed to the particles was evaluated using the comet assay in its alkaline version, as described previously [38]. After exposure to particles, cells were collected using trypsin and stored at -80°C in freezing buffer (85.5 g/L sucrose, 50 ml/L DMSO prepared in citrate buffer (11.8 g/L), pH 7.6). Ten thousand cells were mixed with 0.6% low melting point agarose (LMPA) and two drops of this mix were deposited on a slide that was previously coated with agarose. The cell/LMPA mix was allowed to solidify on ice for 10 min, then slides were immersed in cold lysis buffer (2.5 M NaCl, 100 mM EDTA, 10 mM Tris, 10% DMSO, 1% Triton X-100, pH10) and incubated overnight at 4°C. Slides were then rinsed with PBS, then DNA was allowed to unwind for 30 min in the electrophoresis buffer (300 mM NaOH, 1 mM EDTA, pH > 13). Electrophoresis was performed in a vertical electrophoresis tank (Cleaver Scientific) at 0.7 V/cm for 30 min. Slides were then neutralized in PBS and stained with 50 μL of GelRed (Thermofisher Scientific). Analysis consisted in recording the % tail DNA on 50 cells per gel using the Comet IV software (Perceptive Instruments, Suffolk, UK). Experiments were repeated three times independently, with two technical replicates per condition in each independent experiment. Cells exposed for 24 h to 100 μM of methyl methanesulfonate were used as positive control, and one control slide exposed to H_2O_2 was used as positive control for the electrophoretic migration.

3. Results

After characterizing the three cobalt-based pigments and determining their respective LD20, we chose to compare the effects of pigments on J774 macrophages and present the results corresponding to the two schemes of exposure tested. The acute effects of cobalt-based pigments were compared to recovery exposure in order to visualized specific persistent effects. For the two schemes of exposures, corundum control was used in order to distinguish the effects due to the internalization of particles or the specificities of the physico-chemical characteristics of the materials composing the pigments tested.

3.1. Physical pigment characterization

The size (hydrodynamic diameter) and the size distribution (polydispersity percentage) of pigments in suspension were characterized using DLS. Size distribution is deemed monodisperse when it is less than 15%. The results in Figure 1A show a high diversity of sizes for all pigments tested. Consequently, the dispersity cannot be measured. However, the average of hydrodynamic diameter for every pigment tested was very different. Indeed, the average hydrodynamic size of PV14 was approximately 994 nm in H2O medium and 860 nm in DMEM culture medium. For PG19, the size was 196 nm in H2O and 98 nm in DMEM and for PB28 the size was 517 in H2O and 441 in DMEM. The variability of size between DMEM medium and H2O was not significant. TEM microscopy (Figure 1B) confirm a high heterogeneity of size and shape for all particle suspensions (pigments and corundum).

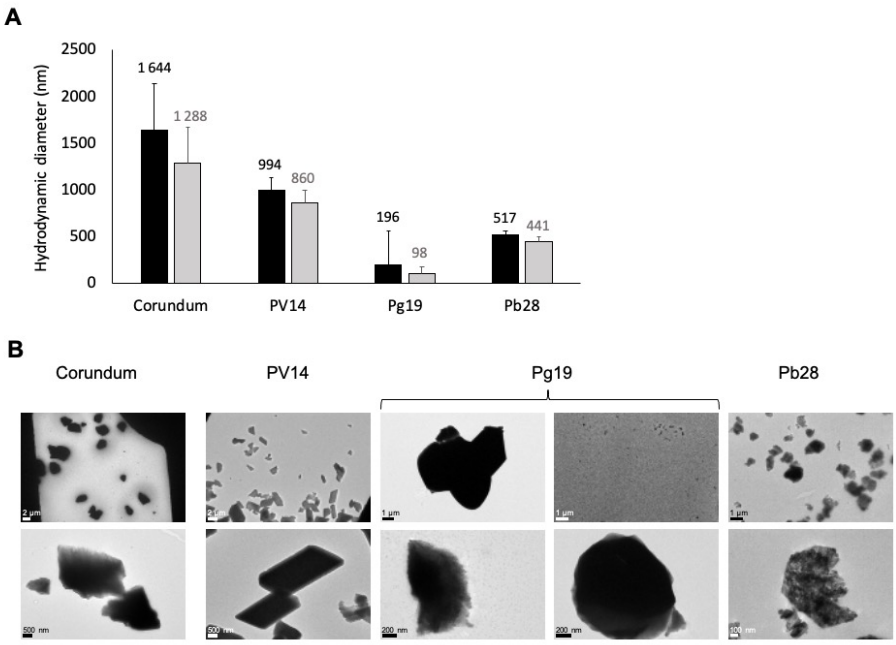

Figure 1 – Characterization of pigments PV14, PG19 and PB28, and their control corundum. Panel A: By DLS in H_2O (in black) and DMEM culture medium (in grey).Panel B: By TEM microscopy in H_2O.

3.2. Chemical pigment characterization

For two of the pigments used in this study, namely Pigment Violet 14 and Pigment Blue 28, the formulas are normally known (respectively cobalt phosphate $Co_3(PO4)_2$ and $CoAl_2O_4$. Pigment Green 19 is described as a mixed cobalt and zinc oxide (Rinmann's green) with undisclosed proportions, so that we had to determine the chemical composition of the pigment. To this purpose, we analyzed the three pigments for their content in aluminium, zinc and cobalt. For comparison purposes, corundum (Al_2O_3 spinel) was included in the analysis, as it has a similar spinel structure as Pigment Blue 28.

The results, shown in Table 1, allow to draw several conclusions

Table 1: metal analysis of the pigments

	Al (µg/l)	Co (µg/l)	Zn(µg/l)
	Measured in mineralisate	**Measured in mineralisate**	**Measured in mineralisate**
Negative control	82.9	0	156
Arabic gum 500 µg/ml	158	0	77.4
Corundum 2.5 µg/ml	90	0	64.5
Corundum 500µg/ml	448	0	129
PV14 2.5µg/ml	92.9	798	76.6
PG19 2.5µg/ml	139	48	1810
PB28 500 µg/ml	2600	641	85.2

First, the mineralization/measurement efficiency of Pigment Violet 14 was around 60%. Second, the mineralization/measurement efficiency of the spinels (both corundum and Pigment Blue 28) was very low, below 1%.
Third, the mineralization/measurement efficiency of Pigment Green 19 was close to quantitative (92% yield) and allowed to determine the relative proportion of zinc and cobalt in the pigment. Thus, the pigment used in this study could be described as $Co_{0.028}Zn_{0.972}O$.

3.3. Determination of pigment dose for cellular assays

To carry out the following functional tests, it was necessary to determine the concentration of pigments allowing to obtain the best compromise between good viability and observation of biological effects. This is why we decided to keep at the lethal dose 20 (LD 20) or just below in order to avoid overmortality in case of variation around this dose, which is likely because of the particular nature of the pigments. Because nanoparticles are known to interfere with many viability estimation methods [39] we chose a dye exclusion method. From the data displayed in Figure 2, we considered that the optimal dose was 2.5 μg/ml for PV14 and PG19, and 500 μg/ml for PB28.

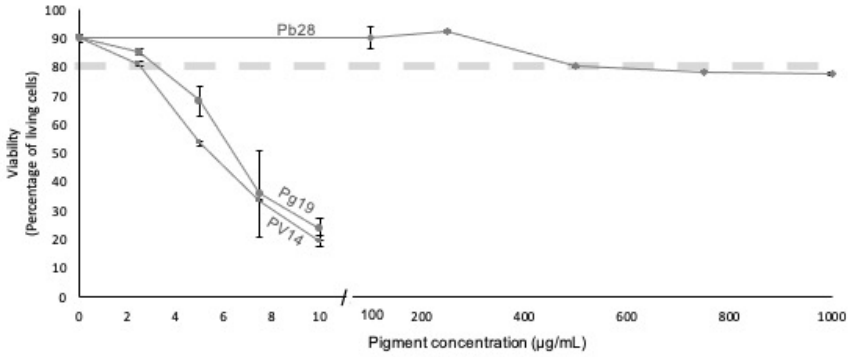

Figure 2 – Viability of J774 cells.
Cells were exposed for 24h to variable doses of pigments (PV14, PG19 and PB28). Viability was measured using propidium iodide (1μg/ml).

3.4. Internalization ability

3.4.1. Measurement of phagocytic activity

To determine whether the pigments induce changes to the main functions of macrophages, a phagocytosis assay was carried out for acute and recovery exposure. The results in Figure 3A and 3C) showed that PV14 (2,5 μg/ml) induced no modification of the proportion of phagocytic cells and of the intensity of fluorescence of phagocytosis-positive cells (MFI) in comparison to corundum (2,5 μg/ml) control. For PG19 (2,5 μg/ml) and, in comparison to corundum (2,5μg/ml), the proportion of the phagocytic cells and the MFI decreased by 38 % and 41 % respectively solely after 72h recovery exposure and not at 24h acute exposure (Figure 3A and 3C). Thus, long and persistent effects on the phagocytic activity was observed for the PG19 pigment. In acute exposure, the result presents in the Figure 3B and 3D showed that PB28 and the Corundum control (500μg/ml) induced a significant decrease of the phagocytic cell (-22 % and -28 % respectively) and a lower decrease on the MFI (-13% and -16%) in comparison to control without treatment. No significant differences between the corundum (500μg/ml) and PB28 (500μg/ml) conditions were observed. Therefore, the reduction of the phagocytic activity was due to a high concentration of particles, regardless of the nature of the particular material. These decreases were maintained (perhaps aggravated) only for PB28 (500μg/ml) in recovery exposure. Indeed, the percentage of phagocytic cells declined by 30 % and for MFI by 15 % to 17 % in comparison to controls.

However, the decrease in the MFI observed under both exposure modes may be linked to interference from the pigment with the fluorescence measurement (see Annex). Thus, for PB28, only the persisting effect observed on the proportion of phagocytic cells can be considered as significant and pigment-specific.

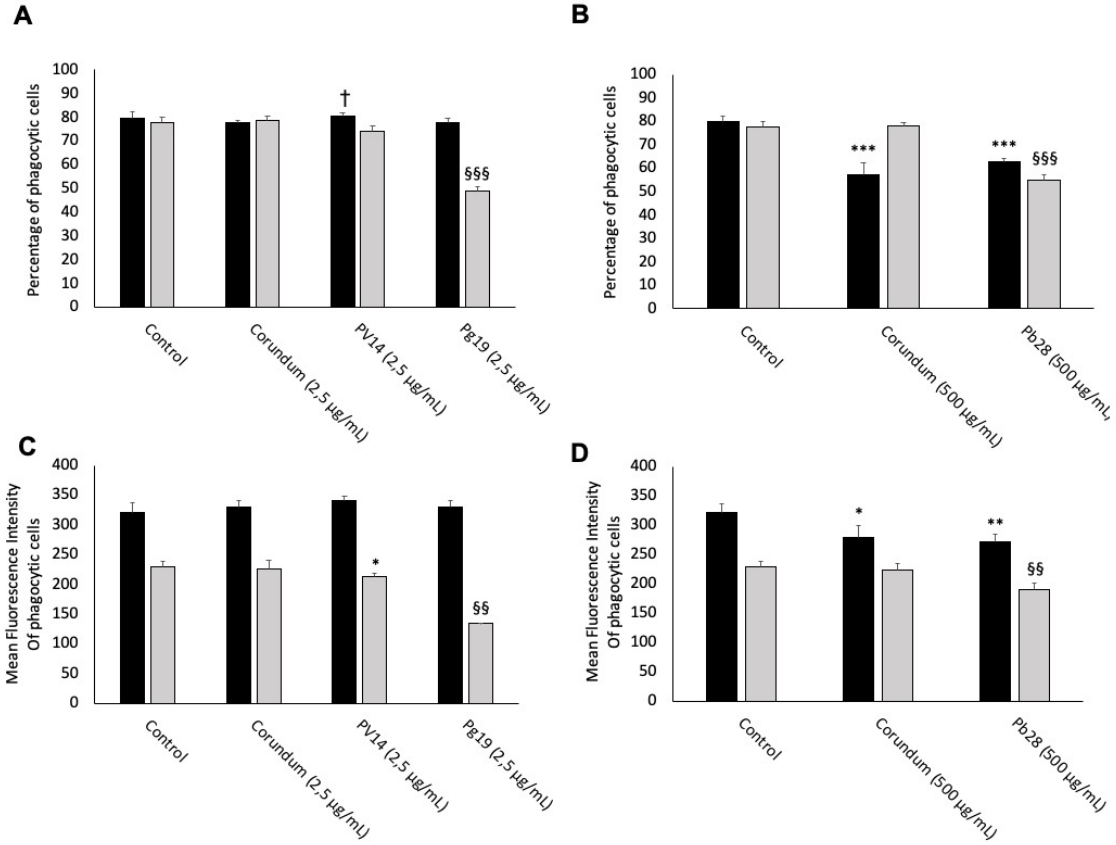

Figure 3 – Phagocytic capacity.
Black bars; acute exposure (24hours). Grey bars: Exposure for 24hours and 3 days recovery post exposure. Panel A: conditions with 2,5 μg/ml of particle suspension. Percentage of cells able to phagocyte fluorescent FITC-labeled latex beads (positive cells). Panel B: conditions with 500 μg/ml of particle suspension. Percentage of cells able to phagocyte fluorescent FITC-labeled latex beads (positive cells). Panel C: conditions with 2,5 μg/ml of particle suspension. Phagocytic ability of positive cells. Panel D: condition with 500 μg/ml of particle suspension. Phagocytic ability of positive cells.
Significance symbols: *: different from negative control only; § different from negative control and corundum control: †: different from corundum control only
Number of symbols: 1: $p<0.05$; 2: $p<0.01$; 3: $p<0.001$

3.4.2. Assessment of lysosomal function

Besides the phagocytic activity, we tested whether pigments altered the lysosomal activity. The neutral red uptake assay allows a crude evaluation of the endosomal and lysosomal activity, as it requires an active proton pump and undamaged lysosomes. The results in Figure 4A and 4B showed no difference regarding the uptake of neutral red between the conditions with and without pigment both for acute and recovery exposure. Thus, no damage to endosomes/lysosomes pathway was observed, confirming that the decrease of phagocytic ability in presence of PB28 (500μg/ml) and corundum (500μg/ml) impacted solely the phagocytosis process without modifying lysosomal integrity.

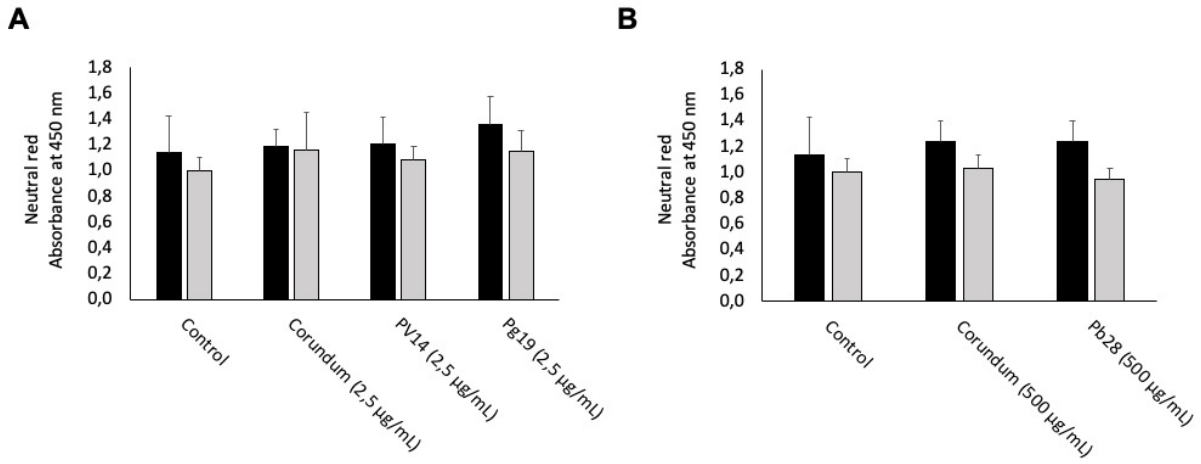

Figure 4 – Neutral red uptake.
Black bars; acute exposure (24hours). Grey bars: Exposure for 24hours and 3 days recovery post exposure. Panel A: conditions with 2,5 μg/ml of particle suspension. Panel B: condition with 500 μg/ml of particle suspension. After elution, the absorbance of the red color released was read at 540 nm.

3.5. Intracellular degradation of the pigments

As the pigments are internalized in large vesicles that can be considered as phagolysosomes, they are exposed to both an acidic and oxidizing environment, which could lead to metal ion release from the pigments into the cells. To evaluate this phenomenon, we measured the soluble ion content of cellular extracts after exposure to the pigments, either at the end of the 24h exposure phase or at the end of the 72h post-exposure period. The results, displayed in Table 2, show distinct differences between the end of the exposure period on the one hand and the end of the exposure period on the other hand.

Table 2: intracellular ion content after exposure to the pigments

	Acute			Recovery		
	Al (ng/mg cellular proteins)	Co (ng/mg cellular proteins)	Zn (ng/mg cellular proteins)	Al (ng/mg cellular proteins)	Co (ng/mg cellular proteins)	Zn (ng/mg cellular proteins)
ctrl	107.7±94.2	254.1±45.7	263.0±109.3	94.9±37.1	121.1±62.5	111.9±30.9
arabic gum 500μg/ml	29.5±35.5	236.0±46.8	153.7±38.0	50.3±30.2	127.8±14.9	80.5±21.5
Corundum 2.5μg/ml	179.3±165.4	320.3±114.0	148.1±53.0	62.9±32.0	112.1±14.2	61.7±21.9
Corundum 500μg/ml	748.7±201*	226.2±15.7	89.6±30.9	116.3±103.9	59.7±72.8	26.0±23.9
PV14 2.5μg/ml	83.0±42.8	541.6±83.9*	120.8±58.6	136.4±177.3	599.2±358.4†	123.3±21.0
PG19 2.5 μg/ml	72.2±32.8	199.4±45.9	315.3±104.8	5.4±9.3	64.8±4.3	68.9±33.6
PB28 500 μg/ml	1191.3±181.9*	360.6±47.2*	120.8±58.6	555.3±295.3†	258.2±59.8†	122.2±38.2

* : significantly different by Student & Mann-Whitney tests
† : significantly different by Mann-Whitney test only

At the end of the exposure period, a significant ion release can be detected for Pigment Violet 14 and Pigment Blue 28. However, this release must be put in perspective with the total metal input. For example, the total input of 1mg Pigment Blue 28 corresponds to 330μg of cobalt, of which only 81ng are detected as intracellular and soluble, i.e. a 0.2% solubilization. Furthermore, the amounts of aluminium and cobalt released from Pigment Blue 28 should be very close, which is not the case in our data, showing that cells do not accumulate passively all ions, but may either solubilize the ions differently or excrete some ions more than others. Pigment Violet 14 appears to be more soluble, with 127 ng of cobalt detected as intracellular and soluble, to be compared to the 2.4 μg of cobalt input, i.e. a 5.3% solubilization.
The results are more difficult to interpret at the end of the recovery period, because the number of cells can be variable from one condition to another, for example because some cells detach from the plate, as indicated by lower protein contents. However, a sustained release of cobalt can be seen from Pigment Violet 14 and from Pigment Blue 28.

3.7. Inflammatory response

The inflammatory response of macrophages was tested with nitric oxide (NO) and cytokine assays. The responses, for all conditions, were assessed in the presence or absence of inflammatory stimuli such as LPS.

3.7.1. Nitric oxide production

We first tested the intrinsic effects of pigments without stimulation with LPS. In acute exposure mode, the results in Figure 5A and 5B show that the production of NO increased significantly for PV14 (2,5μg/ml) in comparison to both control without treatment and corundum control (2,5 μg/ml). Thus, this pro-inflammatory effect was specific to this pigment. In recovery exposure mode, the results were more difficult to interpret. Indeed, results shows a trend toward an enhancement of the secretion of NO under all conditions except PG19. However, the results were never clearly significant in comparison to control without treatment or corundum controls. Thus, we cannot conclude on the specific intrinsic effects of pigments.

After stimulating cells with LPS for the last 18 hours, in acute or recovery exposure modes, the results with pigments obtained in comparison to the condition without particles showed that the secretion of NO remained unchanged for cells exposed to corundum, PB28 and PG19 (Figure 5C and 5D). For PV14 (in acute exposure), we observed a trend toward an increase of the concentration of NO. However, this result must be taken with caution, as the difference was significant only in comparison to corundum control (2,5 μg/ml), not in comparison to control without treatment.

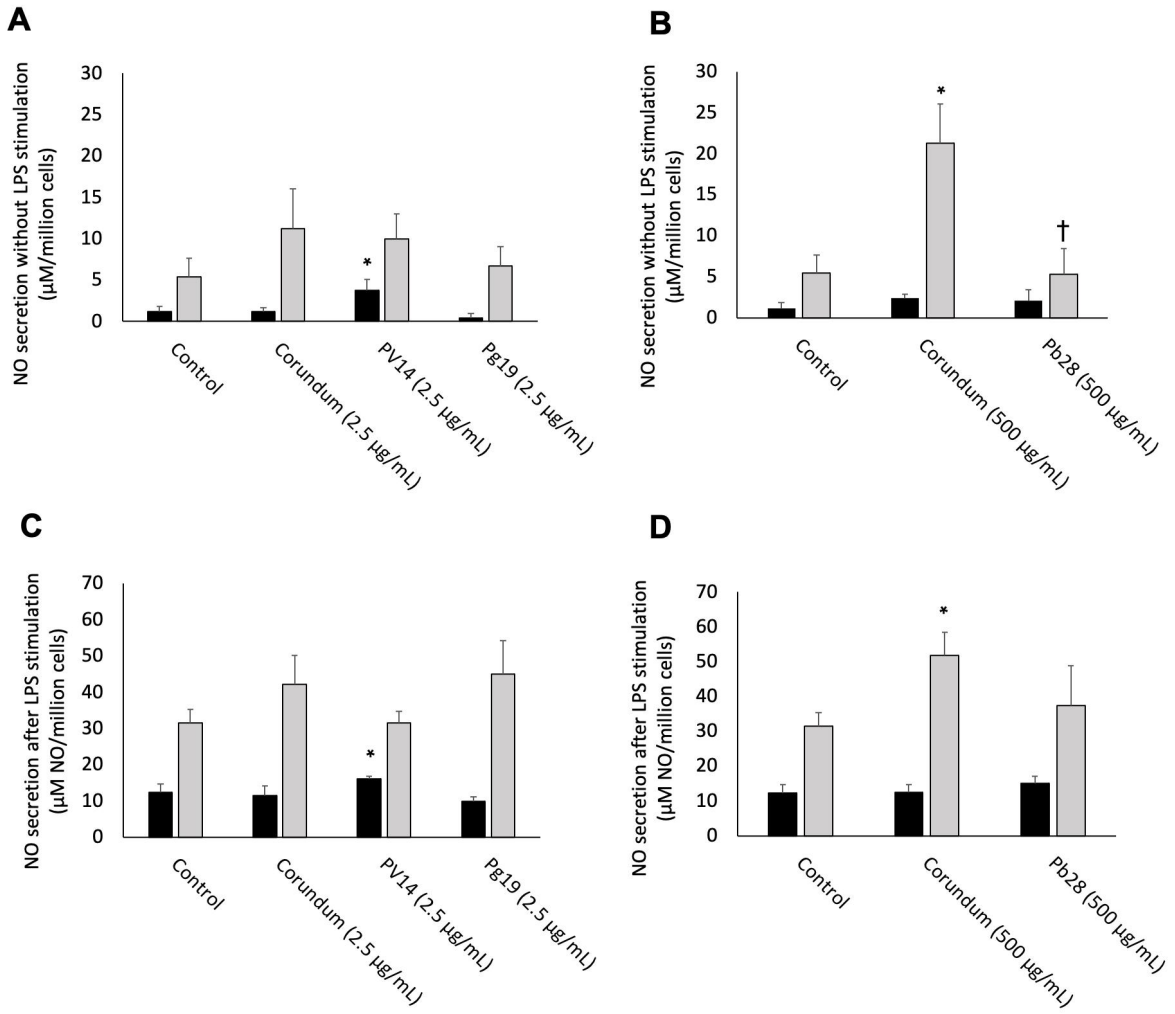

Figure 5 – NO secretion.
Black bars; acute exposure (24hours). Grey bars: Exposure for 24hours and 3 days recovery post exposure. Panel A: NO secretion without LPS stimulation. Conditions with 2,5 μg/ml of particle suspension. Panel B: NO secretion without LPS stimulation. Conditions with 500 μg/ml of particle suspension. Panel C: NO secretion with LPS stimulation Conditions with 2,5 μg/ml of particle suspension. Panel D: NO secretion with LPS stimulation. Condition with 500 μg/ml of particle suspension.
Significance symbols: *: different from negative control only; § different from negative control and corundum control: †: different from corundum control only

3.7.2. Cytokines secretion

In order to determine if pigments induced an intrinsic inflammatory effect, as suggested by the results on nitric oxide, the release of cytokines by cells were measured without LPS stimulation. In acute exposure mode, results in Figure 6A to 6D show that a significant increase of the secretion of TNF and IL-6 for the conditions with particle suspension (comprising pigments) in comparison to cells without treatment. This increase remained however far below the one induced by LPS stimulation. However, only the PV14 condition revealed an additional significant increase of TNF and IL-6 release in comparison to its corundum control (2,5 μg/ml). In recovery exposure mode, the results also show a significant increase in cytokines released with particles suspensions in comparison to control without treatment. Then, in comparison to the respective corundum controls, only the increase of IL-6 for PV14 (2,5 μg/ml) and PB28 (500 μg/ml) were significant.

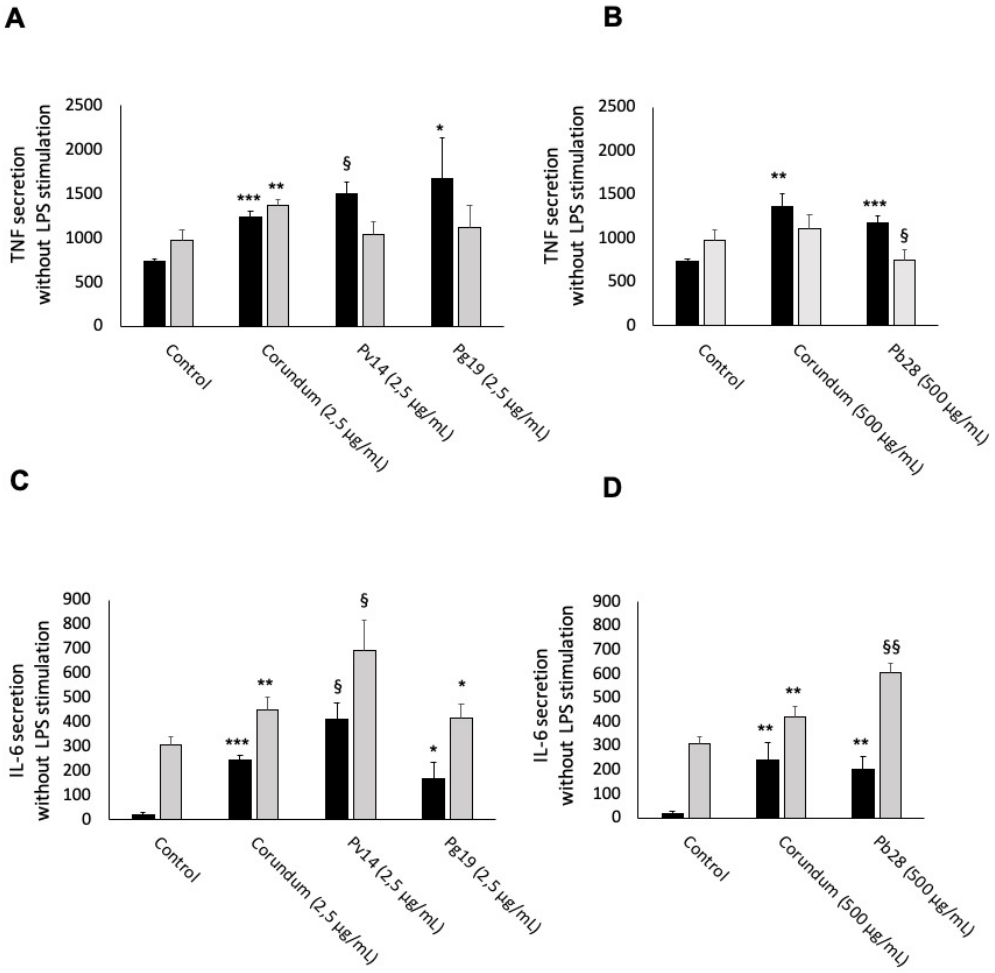

Figure 6 – Cytokines secretion without LPS stimulation
. Black bars; acute exposure (24hours). Grey bars: Exposure for 24hours and 3 days recovery post exposure. Panel A: TNF secretion. Conditions with 2,5 μg/ml of particle suspension. Panel B: TNF secretion. Conditions with 500 μg/ml of particle suspension. Panel C: IL-6 secretion. Conditions with 2,5 μg/ml of particle suspension. Panel D: IL-6 secretion. Condition with 500 μg/ml of particle suspension.
Significance symbols: *: different from negative control only; § different from negative control and corundum control: †: different from corundum control only.
Number of symbols: 1: $p<0.05$; 2: $p<0.01$; 3: $p<0.001$

Following LPS stimulation, in acute exposure mode, pro-inflammatory cytokine assays (Figure 7) revealed no significant differences of TNF and IL-6 secretion for all conditions in comparison to control without treatment and their respective corundum controls. These results suggest that pigments induce no change concerning the capacity of macrophages to release TNF and IL-6 in response to a bacterial stimulus. However, in recovery exposure mode, results in Figure 7A and 7B show that a significant decrease of TNF secretion for pigment and corundum controls in comparison to control without treatment. These results suggest a delayed effect of particles that cannot be detected immediately after exposure. Then, TNF secretion significantly dropped by 65,6 %, 67,4 % and 89,5 % with the three cobalt pigments (PV14, PG19 and PB28) in comparison to their respective corundum controls (2,5 μg/ml or 500 μg/ml). this additional reduction is thus specific to pigments and not exclusively linked to particles internalization. In Figure 7D, for IL-6 secretion, the decrease is only observed, in a

lesser extend for corundum (500μg/ml) and PB28 (500 μg/ml) due to the high concentration of particles independently from their material composition.

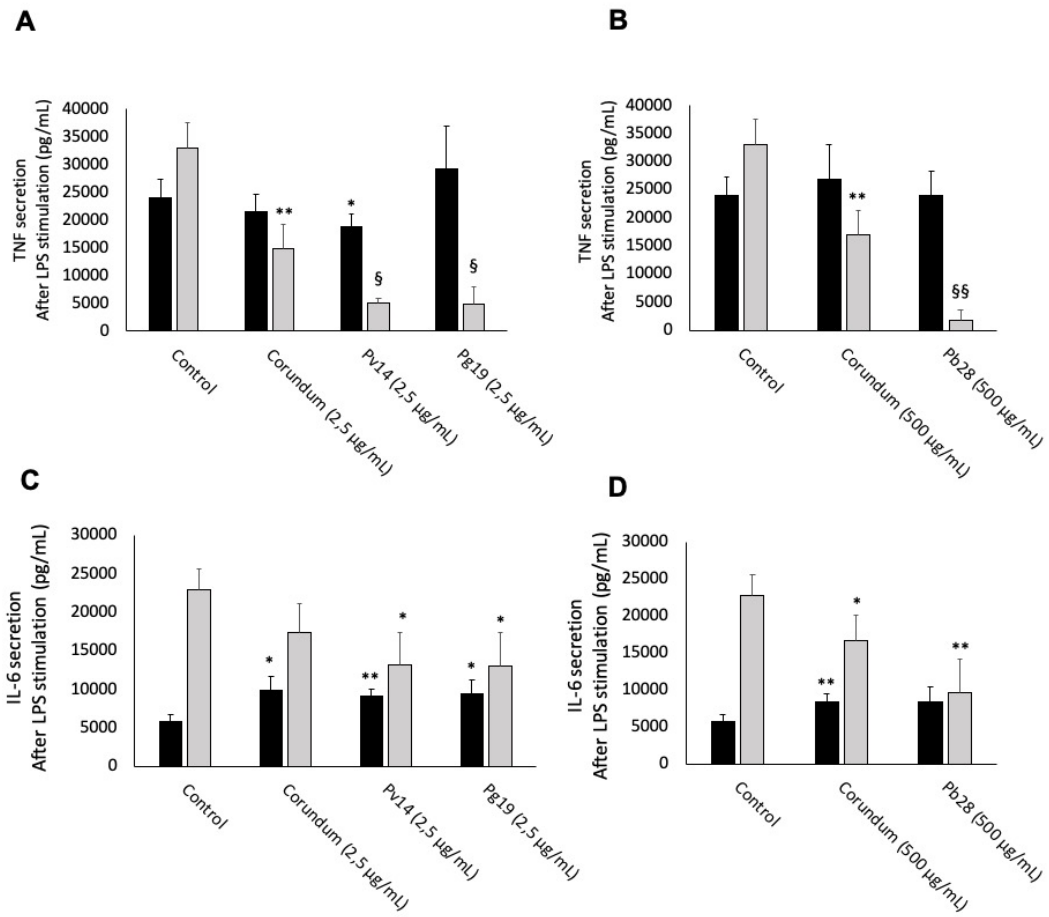

Figure 7 – Cytokines secretion after LPS stimulation.
Black bars; acute exposure (24hours). Grey bars: Exposure for 24hours and 3 days recovery post exposure. Panel A: TNF secretion. Conditions with 2,5 μg/ml of particle suspension. Panel B: TNF secretion. Conditions with 500 μg/ml of particle suspension. Panel C: IL-6 secretion. Conditions with 2,5 μg/ml of particle suspension. Panel D: IL-6 secretion. Condition with 500 μg/ml of particle suspension.
Significance symbols: *: different from negative control only; § different from negative control and corundum control: †: different from corundum control only.
Number of symbols: 1: $p<0.05$; 2: $p<0.01$; 3: $p<0.001$

3.8. Modulation of cell surface markers

In order to know if pigments induced changes in the macrophages profiles, specifics surface markers involved in the immune interactions and polarization were assessed (immunophenotyping).

3.8.1. CD11b

We first screened CD11b, which is an integrin classically associated to macrophages and dendritic cells. We thus investigated the proportion of cells becoming negative for the presence of CD11b at their surface. The results in figure 8A showed that, in acute exposure, no alteration (change) of the CD11b presence on the cell surface in presence of PV14 (2,5

μg/ml) and PG19 (2,5 μg/ml) in comparison to control without treatment or corundum control (2,5 μg/ml). However, we observed a significant slight increase of CD11b negative cells with a higher concentration of corundum (500 μg/ml) (Figure 8B). Moreover, the percentage of CD11b negative cells increased dramatically with PB28 (500 μg/ml), even in comparison with its corundum control (500 μg/ml) (Figure 8B).
This increase of the proportion of CD11b-negative cells was present at the end of the recovery period, both for high concentrations of corundum and PB28, suggesting sustained effects (Figure 8B). It also became significant after recovery for cells exposed to PV14 or PG19 (Figure 8A), although in lesser proportion that for cells exposed to PB28, suggesting in this case a delayed effect.

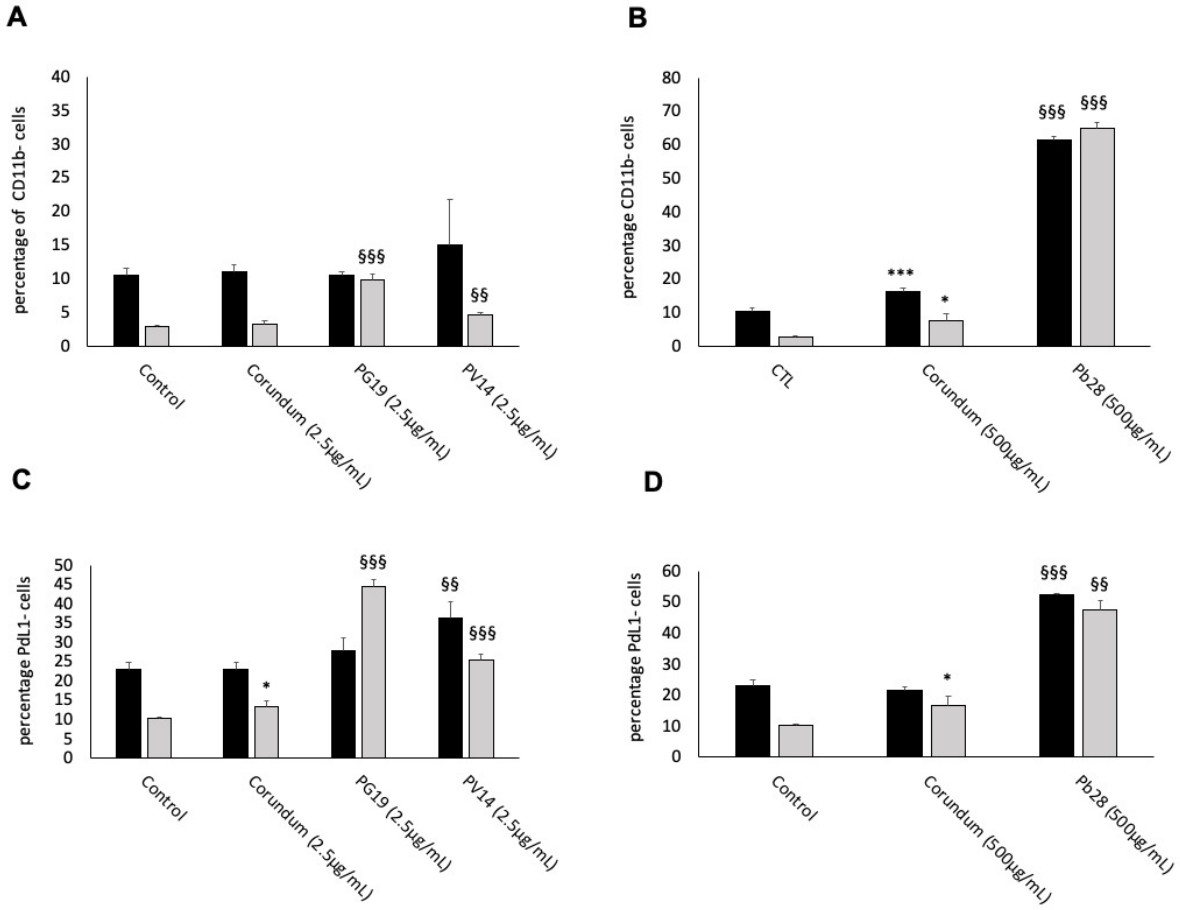

Figure 8 – CD11b and PdL1 cell surface marking. Panel A: Percentage of CD11b- cells in comparison to unlabeled control cells. Conditions with 2,5 μg/ml of particle suspension. Panel B: Percentage of CD11b- cells in comparison to unlabeled control cells. Conditions with 500 μg/ml of particle suspension. Panel C: Percentage of PdL1- cells in comparison to unlabeled control cells. Conditions with 2,5 μg/ml of particle suspension. Panel D: Percentage of PdL1- cells in comparison to unlabeled control cells. Conditions with 500 μg/ml of particle suspension
Significance symbols: *: different from negative control only; § different from negative control and corundum control: †: different from corundum control only.
Number of symbols: 1: $p<0.05$; 2: $p<0.01$; 3: $p<0.001$

3.8.2. Pd-L1

PdL-1 is known to be a surface marker mediating immunomodulation by the inactivation of T cells responses, and is normally expressed at high levels by macrophages [40]. There is however a proportion of cells that express low levels of PdL-1 [41], and we measured the evolution of this proportion following exposure to pigments and corundum. In the acute exposure mode, corundum did not show any effects at low or high concentration, and PG19

did not show any effect either (Figure 8C, D). However, exposure to PV14 or PB28 showed an increase in the proportion of PDL1-negative cells after acute exposure (Figure 8C, D). After the recovery period, the exposure to corundum led to a small but significant increase in the proportion of PDL1-negative cells, while the exposure to all pigments led to a much higher increase in the proportion of PDL1-negative cells (Figure 8C, D), peaking to 50% for cells exposed to PB28.

3.8.3. CD206

CD206 is a surface marker overexpressed on M2 macrophages, and is used as a marker for an anti-inflammatory profile. As its expression is always low, we focused in this case on the intensity of the expression rather than on proportions of positive or negative cells. In the acute exposure mode, the MFI increased significantly only for PG19 (about 30 %) in comparison to both control without treatment and corundum (2,5 μg/ml). However, this is not maintained at the end of recovery exposure. Moreover, the results showed a significant delayed effect of PV14 (Figure 9A). No effects were detected after exposure to corundum or PB28 in both modes.

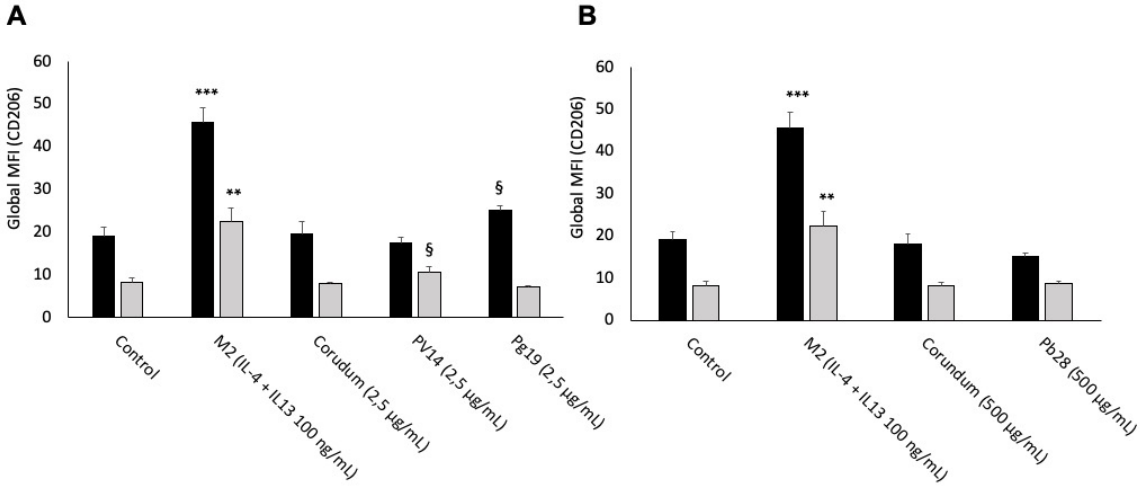

Figure 9-CD206 surface marker (M2 macrophages) Panel A: Global MFI of CD206 in comparison to unlabeled control cells. Conditions with 2,5 μg/ml of particle suspension. Panel B: Global MFI of CD206 in comparison to unlabeled control cells. Conditions with 500 μg/ml of particle suspension.
Significance symbols: *: different from negative control only; § different from negative control and corundum control.
Number of symbols: 1: $p<0.05$; 2: $p<0.01$

3.9. Genotoxicity

As cobalt is known to be genotoxic [28]], we investigated this hypothesis and tested it by a comet assay. The results, shown in Figure 10, indicated no effects of corundum or pigments at the low concentration (2.5μg/ml), neither immediately after exposure nor after the recovery period. However, a significant increase in DNA damage was observed immediately after exposure to high concentrations of particles (either corundum or PB28). The effect disappeared at the end of the recovery period for corundum, but not for PB28, in which a sustained effect was detected, although less intense than just after exposure.

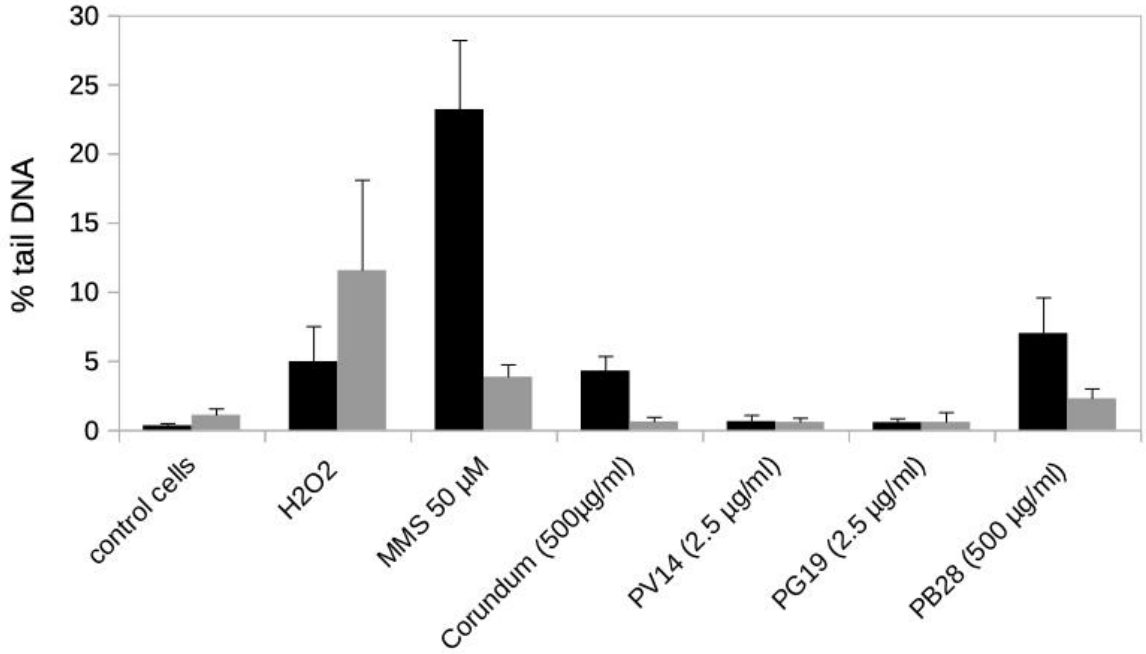

Figure 10-Genotoxicity as determined by a comet assay
The percentage of DNA in the comet tail is measured as an indicator of the extent of DNA damage. Methyl methane sulfonate MMS and hydrogen peroxide are used as positive controls
Significance symbols: *: different from negative control only; § different from negative control and corundum control.
Number of symbols: 1: $p<0.05$; 2: $p<0.01$

4. Discussion

In the context of a use in tattoos, the first question to be addressed is the relevance of the dose to be tested. The injected dose of pigments has been reported to be in the 0.5-9 mg/cm2, with an estimated mean of 2.5 mg/cm2 [9]. If it is assumed that all of this pigment dose is finally collected by the dermal macrophages [14,15], then this surface dose can be transposed to the pure macrophage culture. When transposed to a 12-well plate with 1 ml of culture medium per well and a culture area of 3.8 cm2, this yields to a dose close to 9.5 mg/ml of pigments. Metal analysis of tattoo inks have suggested that they often contain a mixture of pigments [24], so that the total pigment dose cannot be considered to be made by only one pigment. But even when taking into account this dilution phenomenon, the doses used in the present study shall not be considered as grossly exaggerated.

Because tattoo inks represent a poorly-regulated field, their composition under the same trade name may evolve over time. In this respect, the comparison of metal contents in tattoo inks between 2009 and 2020 [24,25] shows a reduction in the toxic metal contents, and for example in the cobalt content. This positive trend shall not hide the fact that the inks used in the early 2000's on people that were around 20 years of age are to be present for still a few decades in the tattooed people.

Thus the interest of examining the effects of cobalt pigments on macrophages cannot be discarded. Although often more expensive than organic pigments, mineral pigments show a

high resistance to light, and degrade only by releasing their constituent metal ions, opposite to organic pigments that can show complex degradation pathways (e.g. in [42,43]).

With the above considerations in mind, we decided to investigate the responses of macrophages to three different cobalt-based pigments. Their toxicity clearly split between toxic pigments (Pigment Violet 14, Pigment Green 19) and pigments of low toxicity (Pigment Blue 28). As the latter could be used at high concentrations (i.e. close to 1 mg/ml) the possibility of a macrophage overload phenomenon [44,45] could not be ruled out. In any case, compared to the untreated negative control, the onset of phagocytosis due to the presence of particulate material is likely to induce changes in macrophage physiology, which shall not be mistaken for specific effects of the cobalt pigments. We thus used the negative control corundum [46] at both low and high concentrations, in order to take into account these potential effects.

Furthermore, as the adverse effects of cobalt can be expected to occur via a progressive release of cobalt ion, we decided to take into account this parameter by using an exposure-recovery scheme, where degradation of the pigments inside the macrophage is likely to start to occur even for poorly-degradable pigments. For more degradable pigments, this degradation may occur even during the exposure period.

Indeed, one of the bases for the low toxicity of pigments resides in their very low solubility in water, and thus by extension in biological media, so that no release of toxic components should occur. Mineral pigments known to be toxic such as lead white (lead basic carbonate) and vermillion (mercuric sulfide) dissolve slowly in biological media, leading to release of toxic heavy metal ions. In fact, biological media are more complex than just water. Assuming that pigments particles end up, at least in part, in macrophages phagolysomes, these particles will encounter a mildly acidic medium (pH 5) containing a high concentration of proteins that bind many metal ions with high affinity. This may explain why water-insoluble pigments may prove soluble to some extent in biological media. This description of the biological media also suggests that pigment biosolubility will depend on the pigment structure.

Our results on cobalt pigments show a clear correlation between the results obtained in strongly acidic mineralization and the results obtained in vivo. Pigments and mineral that poorly solubilize in acidic media, such as corundum or PB28, are also dissolved in the cells with a low efficiency (0.2% after 24 hours) while pigments that dissolve more easily in acidic media such as PV14 also dissolve more easily in the cells (5% dissolved in the cells after 24 hours). This reflects in the toxicity of the pigments, as more soluble pigments show a higher toxicity than poorly soluble pigments (LD20 of 2.5 μg/ml for PV14 compared to 500μg/ml for PB28). The data are more difficult to interpret for PG19, as its cobalt content is very low and thus indistinguishable from the background levels.

Because of this differential solubility, the biological effects of the pigments are likely to be a mixture of pure particular effects and of effects linked to ion release. This is why we systematically included corundum as a particular control, as it had been shown to exhibit minimal toxicity and no pro-inflammatory effects, which are of great interest to be studied in macrophage biology [46].

One of the effects that can be expected to be dependent on the particles concentration is phagocytosis, linked to the well known overload effect [44,45]. Our results correlated well with this model, as no impact on phagocytosis was detected for low particle loads, while an impact was detected at high particle load. Interestingly, cells highly loaded with corundum did recover a normal phagocytic activity after a few days, while cells exposed to an equal concentration of a cobalt-containing pigment with the same crystalline structure (spinel) did not, showing a clear effect of cobalt.

All particles also induced a weak pro-inflammatory effect, even corundum, for which this effect had not been detected previously in an indirect assay, but in serum-free culture conditions [46]. For TNF this effect was essentially transient and of low amplitude. However, a decrease could be noted after recovery for the cells exposed to PB28 at high concentration, probably linked to cobalt release.

This scheme was not observed for interleukin 6, for which a sustained stimulation was observed for all particles, in line with what has been described previously for silica [33] or for silver nanowires [47].

To go further in the intrinsic effects of cobalt-containing pigments on macrophages, we also investigated their genotoxicity. Interestingly, the highly soluble and toxic pigments did not show a detectable genotoxicity, even though the intracellular soluble cobalt content is far above the concentration used as soluble cobalt on total leukocytes (100-200 fg Co/cell in this work, based on a protein content of 300pg protein/cell [48], compared to the 5-8 fg Co/cell used on leukocytes) [28]. This result is in line with the known resistance of macrophages to genotoxicity, opposite to the sensitivity of lymphocytes that account for the vast majority of mononuclear leukocytes. Interestingly, a genotoxic effect was found with high concentrations of particles, either corundum or PB28. This effect was transient for corundum but sustained for PB28. This effect may be correlated either with the release of soluble aluminium (Table 2), or with an intrinsic effect of some insoluble particles, as also described for titanium dioxide (reviewed in [49]).

In addition to these effects, we investigated other effects of the cobalt-containg pigments on the functionality of macrophages. We first investigated the response to an LPS-challenge, which would mimick an antibacterial response. While a small but significant increase in the IL-6 secretion could be noted immediately after exposure, the most striking fact is the general decrease in the TNF and IL-6 responses after the recovery period. Coupled with the effects on phagocytosis, these results suggest that macrophages become slightly less efficient in fighting a bacterial infection when loaded with cobalt-containing pigments. Such an effect was not observed when macrophages were treated with amorphous silica [33], but was also observed when macrophages were treated with silver nanoparticles [32], which also release toxic metallic ions during the recovery phase. When compared to results obtained upon chronic exposure to silver nanoparticles [50], the results of this study on cobalt-containing pigments suggest that this decrease in performance may last over time, which is to be taken into account in the perspective of long-term effects of tattoos.

Finally, we also tested cell surface markers relevant for the fine functioning of macrophages, namely CD11b, PdL-1 and CD206. CD206 is one of the hallmarks for M2 macrophages, which are associated to wound healing but also to tumor progression [51]. Only PV14 after the recovery period showed a slight tendency toward an increase of CD206, and thus an increased polarization toward the M2 phenotype, keeping in mind that macrophage polarization shall be viewed as a continuum [52]. PdL-1 is a surface protein involved in cell-cell interactions in the immune system, and seems to play a role in suppressing immune responses. As such, a high expression of PdL-1 has been implicated in tolerance, e.g. in the eye [53], but also associated with immunodeficiency in atherosclerotic patients [41]. Oppositely, PdL-1 low cells have been implicated in intestinal inflammation [41]. Our results clearly show a major increase in PdL-1 low cells when cells are treated with cobalt-containing pigments, and this phenotype seems sustained over time. Thus, macrophages loaded with cobalt-containing pigments may decrease the tolerant phenotype that is encountered in tissue-resident macrophages [54], increase their proliferation and their pro-inflammatory activity [55], maybe through their interaction with other immune cells of the skin [56], which might lead to a form of chronic inflammation.

This hypothesis is further reinforced by the results that we obtained on CD11b, where an increase in the proportion of CD11b-negative cells was noted (Figure 8). First of all, CD11b

is an integrin [57], and as such plays a role in the adhesion of the macrophages to their substrate. Thus, it is not surprising that the proportion of CD11b-negative cells decreases during the recovery period in the control condition. CD11b-negative being probably less adherent, they are likely to be more easily lost upon culture medium changes. As a first consequence, the increase in the proportion of CD11b-negative cells observed after treatment with cobalt-containing pigments may translate into a higher propensity of these cells to leave their initial site, i.e. the dermis, and migrate, for example in the lymph nodes, where pigment-loaded cells have been observed in tattooed individuals [18].

Furthermore, CD11b is also part of the complement receptor 3, and plays as such a role in phagocytosis for complement-opsonized pathogens [58]. Thus, CD11b-negative cells are likely to be impaired in this pathway, and thus efficient for the elimination of pathogens.

Last but not least, CD11b also plays a role in immune regulation, as a negative regulator of immune responses [59,60]. Thus, absence of CD11b results in more active T cell activation [61] and may result in tolerance reduction and over-inflammation [62], a process that appears synergistic with the reduction of PdL-1. In addition, activation of CD11b, which is linked to anti-tumor immune response [63], will be impossible in CD11b-negative cells, and may contribute to lower anti-tumoral activity.

Overall and population-wise, the macrophages treated with cobalt-containing pigments appear less competent against pathogens, less competent against tumors and with a more pro-inflammatory phenotype, beyond the simple production of cytokines. Of course the effects are likely to be moderate, and it can be argued that the effects that we detected over a few days may normalize over time. However, our results on the persistence of the effects, coupled with the now established capture-death-recapture macrophage cycle with tattoo pigments [14,15], are more in favor of a self-sustaining process altering macrophages on the long term.

Although cobalt pigments are now of rare use in tattoo inks, the fact that people may have received such pigments in the past [24], coupled with the possibility that other pigments may also alter macrophages functions, maybe by completely different mechanisms, deserves in our opinion more research.

5. References

1. Deter-Wolf, A. The Material Culture and Middle Stone Age Origins of Ancient Tattooing. In *Tattoos and Body Modifications in Antiquity. Proceedings of the sessions at the EAA annual meetings in The Hague and Oslo, 2010/11*; Zurich Studies in Archaeology; 2013; pp. 15–26.
2. Dorfer, L.; Moser, M.; Bahr, F.; Spindler, K.; Egarter-Vigl, E.; Giullén, S.; Dohr, G.; Kenner, T. A Medical Report from the Stone Age? *Lancet* **1999**, *354*, 1023–1025, doi:10.1016/S0140-6736(98)12242-0.
3. Pabst, M.A.; Letofsky-Papst, I.; Moser, M.; Spindler, K.; Bock, E.; Wilhelm, P.; Leopold Dorfer, M.D.; Geigl, J.B.; Auer, M.; Speicher, M.R.; et al. Different Staining Substances Were Used in Decorative and Therapeutic Tattoos in a 1000-Year-Old Peruvian Mummy. *Journal of Archaeological Science* **2010**, *37*, 3256–3262, doi:10.1016/j.jas.2010.07.026.
4. Maarouf, M.; Saberian, C.; Segal, R.J.; Shi, V.Y. A New Era For Tattoos, with New Potential Complications. *J Clin Aesthet Dermatol* **2019**, *12*, 37–38.
5. Paprottka, F.J.; Krezdorn, N.; Narwan, M.; Turk, M.; Sorg, H.; Noah, E.M.; Hebebrand, D. Trendy Tattoos-Maybe a Serious Health Risk? *Aesthetic Plast Surg* **2018**, *42*, 310–321, doi:10.1007/s00266-017-1002-0.
6. Jacob, C.I. Tattoo-Associated Dermatoses: A Case Report and Review of the Literature. *Dermatol Surg* **2002**, *28*, 962–965, doi:10.1046/j.1524-4725.2002.02066.x.
7. Forbat, E.; Al-Niaimi, F. Patterns of Reactions to Red Pigment Tattoo and Treatment Methods. *Dermatol Ther (Heidelb)* **2016**, *6*, 13–23, doi:10.1007/s13555-016-0104-y.
8. Lerche, C.M.; Heerfordt, I.M.; Serup, J.; Poulsen, T.; Wulf, H.C. Red Tattoos, Ultraviolet Radiation and Skin Cancer in Mice. *Exp Dermatol* **2017**, *26*, 1091–1096, doi:10.1111/exd.13383.
9. Baumler, W. Absorption, Distribution, Metabolism and Excretion of Tattoo Colorants and Ingredients in Mouse and Man: The Known and the Unknown. In *Current Problems in Dermatology*; Serup, J., Kluger, N., Baumler, W., Eds.; S. Karger AG, 2015; Vol. 48, pp. 176–184 ISBN 978-3-318-02776-1.
10. Regensburger, J.; Lehner, K.; Maisch, T.; Vasold, R.; Santarelli, F.; Engel, E.; Gollmer, A.; König, B.; Landthaler, M.; Bäumler, W. Tattoo Inks Contain Polycyclic Aromatic Hydrocarbons That Additionally Generate Deleterious Singlet Oxygen. *Exp Dermatol* **2010**, *19*, e275-281, doi:10.1111/j.1600-0625.2010.01068.x.
11. Kluger, N.; Koljonen, V. Tattoos, Inks, and Cancer. *Lancet Oncol* **2012**, *13*, e161-168, doi:10.1016/S1470-2045(11)70340-0.
12. Wenzel, S.M.; Rittmann, I.; Landthaler, M.; Bäumler, W. Adverse Reactions after Tattooing: Review of the Literature and Comparison to Results of a Survey. *Dermatology* **2013**, *226*, 138–147, doi:10.1159/000346943.
13. Kluegl, I.; Hiller, K.-A.; Landthaler, M.; Baeumler, W. Incidence of Health Problems Associated with Tattooed Skin: A Nation-Wide Survey in German-Speaking Countries. *Dermatology* **2010**, *221*, 43–50, doi:10.1159/000292627.
14. Baranska, A.; Shawket, A.; Jouve, M.; Baratin, M.; Malosse, C.; Voluzan, O.; Vu Manh, T.-P.; Fiore, F.; Bajénoff, M.; Benaroch, P.; et al. Unveiling Skin Macrophage Dynamics Explains Both Tattoo Persistence and Strenuous Removal. *J Exp Med* **2018**, *215*, 1115–1133, doi:10.1084/jem.20171608.
15. Collin, M. Death, Eaters, and Dark Marks. *J Exp Med* **2018**, *215*, 1005–1006, doi:10.1084/jem.20180311.
16. Chen, G.Y.; Nuñez, G. Sterile Inflammation: Sensing and Reacting to Damage. *Nat Rev Immunol* **2010**, *10*, 826–837, doi:10.1038/nri2873.
17. Navegantes, K.C.; de Souza Gomes, R.; Pereira, P.A.T.; Czaikoski, P.G.; Azevedo, C.H.M.; Monteiro, M.C. Immune Modulation of Some Autoimmune Diseases: The Critical Role of Macrophages and Neutrophils in the Innate and Adaptive Immunity. *J Transl Med* **2017**, *15*, 36, doi:10.1186/s12967-017-1141-8.

18. Schreiver, I.; Hesse, B.; Seim, C.; Castillo-Michel, H.; Villanova, J.; Laux, P.; Dreiack, N.; Penning, R.; Tucoulou, R.; Cotte, M.; et al. Synchrotron-Based v-XRF Mapping and µ-FTIR Microscopy Enable to Look into the Fate and Effects of Tattoo Pigments in Human Skin. *Sci Rep* **2017**, *7*, 11395, doi:10.1038/s41598-017-11721-z.
19. Nopajaroonsri, C.; Simon, G.T. Phagocytosis of Colloidal Carbon in a Lymph Node. *Am J Pathol* **1971**, *65*, 25–42.
20. Engel, E.; Vasold, R.; Santarelli, F.; Maisch, T.; Gopee, N.V.; Howard, P.C.; Landthaler, M.; Bäumler, W. Tattooing of Skin Results in Transportation and Light-Induced Decomposition of Tattoo Pigments--a First Quantification in Vivo Using a Mouse Model. *Exp Dermatol* **2010**, *19*, 54–60, doi:10.1111/j.1600-0625.2009.00925.x.
21. Lehner, K.; Santarelli, F.; Penning, R.; Vasold, R.; Engel, E.; Maisch, T.; Gastl, K.; König, B.; Landthaler, M.; Bäumler, W. The Decrease of Pigment Concentration in Red Tattooed Skin Years after Tattooing. *J Eur Acad Dermatol Venereol* **2011**, *25*, 1340–1345, doi:10.1111/j.1468-3083.2011.03987.x.
22. Khan, Z.; Combadière, C.; Authier, F.-J.; Itier, V.; Lux, F.; Exley, C.; Mahrouf-Yorgov, M.; Decrouy, X.; Moretto, P.; Tillement, O.; et al. Slow CCL2-Dependent Translocation of Biopersistent Particles from Muscle to Brain. *BMC Med* **2013**, *11*, 99, doi:10.1186/1741-7015-11-99.
23. Gherardi, R.K.; Eidi, H.; Crépeaux, G.; Authier, F.J.; Cadusseau, J. Biopersistence and Brain Translocation of Aluminum Adjuvants of Vaccines. *Front Neurol* **2015**, *6*, 4, doi:10.3389/fneur.2015.00004.
24. Forte, G.; Petrucci, F.; Cristaudo, A.; Bocca, B. Market Survey on Toxic Metals Contained in Tattoo Inks. *Science of The Total Environment* **2009**, *407*, 5997–6002, doi:10.1016/j.scitotenv.2009.08.034.
25. Battistini, B.; Petrucci, F.; De Angelis, I.; Failla, C.M.; Bocca, B. Quantitative Analysis of Metals and Metal-Based Nano- and Submicron-Particles in Tattoo Inks. *Chemosphere* **2020**, *245*, 125667, doi:10.1016/j.chemosphere.2019.125667.
26. Simonsen, L.O.; Harbak, H.; Bennekou, P. Cobalt Metabolism and Toxicology--a Brief Update. *Sci Total Environ* **2012**, *432*, 210–215, doi:10.1016/j.scitotenv.2012.06.009.
27. Papageorgiou, I.; Brown, C.; Schins, R.; Singh, S.; Newson, R.; Davis, S.; Fisher, J.; Ingham, E.; Case, C.P. The Effect of Nano- and Micron-Sized Particles of Cobalt-Chromium Alloy on Human Fibroblasts in Vitro. *Biomaterials* **2007**, *28*, 2946–2958, doi:10.1016/j.biomaterials.2007.02.034.
28. Colognato, R.; Bonelli, A.; Ponti, J.; Farina, M.; Bergamaschi, E.; Sabbioni, E.; Migliore, L. Comparative Genotoxicity of Cobalt Nanoparticles and Ions on Human Peripheral Leukocytes in Vitro. *Mutagenesis* **2008**, *23*, 377–382, doi:10.1093/mutage/gen024.
29. Kwon, Y.-M.; Xia, Z.; Glyn-Jones, S.; Beard, D.; Gill, H.S.; Murray, D.W. Dose-Dependent Cytotoxicity of Clinically Relevant Cobalt Nanoparticles and Ions on Macrophages in Vitro. *Biomed Mater* **2009**, *4*, 025018, doi:10.1088/1748-6041/4/2/025018.
30. Kumanto, M.; Paukkeri, E.-L.; Nieminen, R.; Moilanen, E. Cobalt(II) Chloride Modifies the Phenotype of Macrophage Activation. *Basic Clin Pharmacol Toxicol* **2017**, *121*, 98–105, doi:10.1111/bcpt.12773.
31. Schuster, B.E.; Roszell, L.E.; Murr, L.E.; Ramirez, D.A.; Demaree, J.D.; Klotz, B.R.; Rosencrance, A.B.; Dennis, W.E.; Bao, W.; Perkins, E.J.; et al. In Vivo Corrosion, Tumor Outcome, and Microarray Gene Expression for Two Types of Muscle-Implanted Tungsten Alloys. *Toxicology and Applied Pharmacology* **2012**, *265*, 128–138, doi:10.1016/j.taap.2012.08.025.
32. Dalzon, B.; Torres, A.; Diemer, H.; Ravanel, S.; Collin-Faure, V.; Pernet-Gallay, K.; Jouneau, P.-H.; Bourguignon, J.; Cianférani, S.; Carrière, M.; et al. How Reversible Are the Effects of Silver Nanoparticles on Macrophages? A Proteomic-Instructed View. *Environmental Science: Nano* **2019**, *6*, 3133–3157.
33. Torres, A.; Dalzon, B.; Collin-Faure, V.; Diemer, H.; Fenel, D.; Schoehn, G.; Cianférani, S.; Carrière, M.; Rabilloud, T. How Reversible Are the Effects of Fumed Silica on Macrophages? A Proteomics-Informed View. *Nanomaterials (Basel)* **2020**, *10*, 1939, doi:10.3390/nano10101939.

34. Rabilloud, T. Optimization of the Cydex Blue Assay: A One-Step Colorimetric Protein Assay Using Cyclodextrins and Compatible with Detergents and Reducers. *PLoS One* **2018**, *13*, e0195755.
35. Abel, G.; Szollosi, J.; Fachet, J. Phagocytosis of Fluorescent Latex Microbeads by Peritoneal Macrophages in Different Strains of Mice: A Flow Cytometric Study. *Eur J Immunogenet* **1991**, *18*, 239–45.
36. Triboulet, S.; Aude-Garcia, C.; Carriere, M.; Diemer, H.; Proamer, F.; Habert, A.; Chevallet, M.; Collin-Faure, V.; Strub, J.M.; Hanau, D.; et al. Molecular Responses of Mouse Macrophages to Copper and Copper Oxide Nanoparticles Inferred from Proteomic Analyses. *Mol Cell Proteomics* **2013**, *12*, 3108–3122.
37. Repetto, G.; del Peso, A.; Zurita, J.L. Neutral Red Uptake Assay for the Estimation of Cell Viability/Cytotoxicity. *Nat Protoc* **2008**, *3*, 1125–31.
38. Armand, L.; Tarantini, A.; Beal, D.; Biola-Clier, M.; Bobyk, L.; Sorieul, S.; Pernet-Gallay, K.; Marie-Desvergne, C.; Lynch, I.; Herlin-Boime, N.; et al. Long-Term Exposure of A549 Cells to Titanium Dioxide Nanoparticles Induces DNA Damage and Sensitizes Cells towards Genotoxic Agents. *Nanotoxicology* **2016**, *10*, 913–923, doi:10.3109/17435390.2016.1141338.
39. Kroll, A.; Pillukat, M.H.; Hahn, D.; Schnekenburger, J. Current in Vitro Methods in Nanoparticle Risk Assessment: Limitations and Challenges. *Eur J Pharm Biopharm* **2009**, *72*, 370–377, doi:10.1016/j.ejpb.2008.08.009.
40. Loke, P.; Allison, J.P. PD-L1 and PD-L2 Are Differentially Regulated by Th1 and Th2 Cells. *Proceedings of the National Academy of Sciences* **2003**, *100*, 5336–5341, doi:10.1073/pnas.0931259100.
41. Weyand, C.M.; Berry, G.J.; Goronzy, J.J. The Immunoinhibitory PD-1/PD-L1 Pathway in Inflammatory Blood Vessel Disease. *J Leukoc Biol* **2017**, jlb.3MA0717-283, doi:10.1189/jlb.3MA0717-283.
42. Schreiver, I.; Hutzler, C.; Laux, P.; Berlien, H.-P.; Luch, A. Formation of Highly Toxic Hydrogen Cyanide upon Ruby Laser Irradiation of the Tattoo Pigment Phthalocyanine Blue. *Sci Rep* **2015**, *5*, 12915, doi:10.1038/srep12915.
43. Bauer, E.M.; Scibetta, E.V.; Cecchetti, D.; Piccirillo, S.; Antonaroli, S.; Sennato, S.; Cerasa, M.; Tagliatesta, P.; Carbone, M. Treatments of a Phthalocyanine-Based Green Ink for Tattoo Removal Purposes: Generation of Toxic Fragments and Potentially Harmful Morphologies. *Arch Toxicol* **2020**, *94*, 2359–2375, doi:10.1007/s00204-020-02790-7.
44. Oberdörster, G. Lung Particle Overload: Implications for Occupational Exposures to Particles. *Regul Toxicol Pharmacol* **1995**, *21*, 123–135, doi:10.1006/rtph.1995.1017.
45. Warheit, D.B.; Hansen, J.F.; Yuen, I.S.; Kelly, D.P.; Snajdr, S.I.; Hartsky, M.A. Inhalation of High Concentrations of Low Toxicity Dusts in Rats Results in Impaired Pulmonary Clearance Mechanisms and Persistent Inflammation. *Toxicol Appl Pharmacol* **1997**, *145*, 10–22, doi:10.1006/taap.1997.8102.
46. Wiemann, M.; Vennemann, A.; Sauer, U.G.; Wiench, K.; Ma-Hock, L.; Landsiedel, R. An in Vitro Alveolar Macrophage Assay for Predicting the Short-Term Inhalation Toxicity of Nanomaterials. *J Nanobiotechnol* **2016**, *14*, 16, doi:10.1186/s12951-016-0164-2.
47. Toybou, D.; Celle, C.; Aude-Garcia, C.; Rabilloud, T.; Simonato, J.-P. A Toxicology-Informed, Safer by Design Approach for the Fabrication of Transparent Electrodes Based on Silver Nanowires. *Environmental Science: Nano* **2019**, *6*, 684–694.
48. Tsuboi, A.; Kurotsu, T.; Terasima, T. Changes in Protein Content per Cell during Growth of Mouse L Cells. *Exp Cell Res* **1976**, *103*, 257–261, doi:10.1016/0014-4827(76)90262-7.
49. Carriere, M.; Arnal, M.-E.; Douki, T. TiO2 Genotoxicity: An Update of the Results Published over the Last Six Years. *Mutat Res* **2020**, *854–855*, 503198, doi:10.1016/j.mrgentox.2020.503198.
50. Dalzon, B.; Aude-Garcia, C.; Diemer, H.; Bons, J.; Marie-Desvergne, C.; Pérard, J.; Dubosson, M.; Collin-Faure, V.; Carapito, C.; Cianférani, S.; et al. The Longer the Worse: A Combined Proteomic and Targeted Study of the Long-Term *versus* Short-Term Effects of Silver Nanoparticles on Macrophages. *Environ. Sci.: Nano* **2020**, *7*, 2032–2046, doi:10.1039/C9EN01329F.

51. Shapouri-Moghaddam, A.; Mohammadian, S.; Vazini, H.; Taghadosi, M.; Esmaeili, S.-A.; Mardani, F.; Seifi, B.; Mohammadi, A.; Afshari, J.T.; Sahebkar, A. Macrophage Plasticity, Polarization, and Function in Health and Disease. *J Cell Physiol* **2018**, *233*, 6425–6440, doi:10.1002/jcp.26429.
52. Sica, A.; Mantovani, A. Macrophage Plasticity and Polarization: In Vivo Veritas. *J Clin Invest* **2012**, *122*, 787–795, doi:10.1172/JCI59643.
53. Taylor, A.W.; Ng, T.F. Negative Regulators That Mediate Ocular Immune Privilege. *J Leukoc Biol* **2018**, *103*, 1179–1187, doi:10.1002/JLB.3MIR0817-337R.
54. Davies, L.C.; Jenkins, S.J.; Allen, J.E.; Taylor, P.R. Tissue-Resident Macrophages. *Nat Immunol* **2013**, *14*, 986–995, doi:10.1038/ni.2705.
55. Hartley, G.P.; Chow, L.; Ammons, D.T.; Wheat, W.H.; Dow, S.W. Programmed Cell Death Ligand 1 (PD-L1) Signaling Regulates Macrophage Proliferation and Activation. *Cancer Immunol Res* **2018**, *6*, 1260–1273, doi:10.1158/2326-6066.CIR-17-0537.
56. Heath, W.R.; Carbone, F.R. The Skin-Resident and Migratory Immune System in Steady State and Memory: Innate Lymphocytes, Dendritic Cells and T Cells. *Nat Immunol* **2013**, *14*, 978–985, doi:10.1038/ni.2680.
57. Remold-O'Donnell, E. Regulation of Synthesis of Macrophage Adhesion Molecule, a Heterodimeric Membrane Glycoprotein. *J Immunol* **1988**, *140*, 1244–1249.
58. Vandendriessche, S.; Cambier, S.; Proost, P.; Marques, P.E. Complement Receptors and Their Role in Leukocyte Recruitment and Phagocytosis. *Front. Cell Dev. Biol.* **2021**, *9*, 624025, doi:10.3389/fcell.2021.624025.
59. Han, C.; Jin, J.; Xu, S.; Liu, H.; Li, N.; Cao, X. Integrin CD11b Negatively Regulates TLR-Triggered Inflammatory Responses by Activating Syk and Promoting Degradation of MyD88 and TRIF via Cbl-b. *Nat Immunol* **2010**, *11*, 734–742, doi:10.1038/ni.1908.
60. Ehirchiou, D.; Xiong, Y.; Xu, G.; Chen, W.; Shi, Y.; Zhang, L. CD11b Facilitates the Development of Peripheral Tolerance by Suppressing Th17 Differentiation. *Journal of Experimental Medicine* **2007**, *204*, 1519–1524, doi:10.1084/jem.20062292.
61. Varga, G.; Balkow, S.; Wild, M.K.; Stadtbaeumer, A.; Krummen, M.; Rothoeft, T.; Higuchi, T.; Beissert, S.; Wethmar, K.; Scharffetter-Kochanek, K.; et al. Active MAC-1 (CD11b/CD18) on DCs Inhibits Full T-Cell Activation. *Blood* **2007**, *109*, 661–669, doi:10.1182/blood-2005-12-023044.
62. Zhang, Q.; Lee, W.-B.; Kang, J.-S.; Kim, L.K.; Kim, Y.-J. Integrin CD11b Negatively Regulates Mincle-Induced Signaling via the Lyn-SIRPα-SHP1 Complex. *Exp Mol Med* **2018**, *50*, e439, doi:10.1038/emm.2017.256.
63. Schmid, M.C.; Khan, S.Q.; Kaneda, M.M.; Pathria, P.; Shepard, R.; Louis, T.L.; Anand, S.; Woo, G.; Leem, C.; Faridi, M.H.; et al. Integrin CD11b Activation Drives Anti-Tumor Innate Immunity. *Nat Commun* **2018**, *9*, 5379, doi:10.1038/s41467-018-07387-4.

ANNEX

In order to verify that all effects of pigments observed were due to functional damages on J774 and not due to possible artifact caused by various interactions between experimental regeants and pigments, we performed the following experiments before functional assays.

Firstly, to asses if the opacity of pigments could interfere with the fluorescence-based assays, such as latex beads internalization (for phagocytosis measurement), we incubated cells with fluorescent latex beads (2 hours) before adding pigment during 3 hours. The internalization of the fluorescent reagent e.g. green fluorescent latex beads was thus uniform in all conditions. After adding a particulate suspension, If a decrease was observed, it was not due to cellular alterations but to the opacity of pigments, which blocks the excitation laser or the emission signal. We were thus able to compare fluorescence intensity with and without pigments, which allowed us to conclude that the fluorescence intensity was decreased with cells loaded with corundum (500 µg/mL) and Pb28 (500 µg/mL) pigments (-9 % and -19 % respectively in comparison to control without treatment) (Figure S1). We can conclude that pigments at high doses can interfere with fluorescent beads-based assays in flow cytometry. Thus, during the phagocytosis assays, the decrease of the MFI for corundum (500 µg/mL) and Pb28 (500 µg/mL) observed on positive cells was not due to alterations of the phagocytosis functionalities.

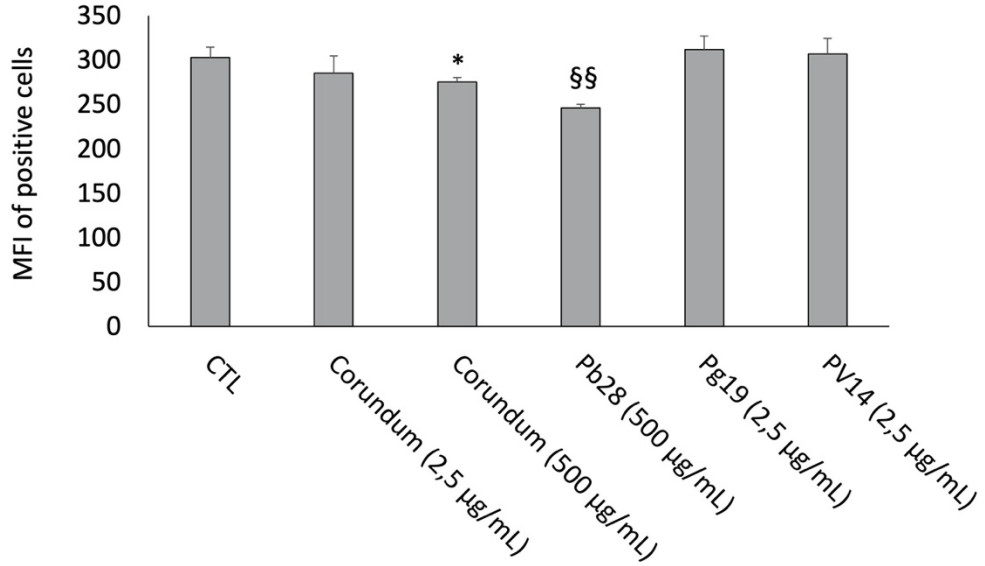

Griess Reagent interference assessment

We also tested interaction between the Griess reaction and pigments. To do so, cells were seeded, let attach for 7 hurs, then arginine and LPS were added and the cells were incubated for a further 18 hours. After the incubation, the supernatants were collected and pigments were added. Then NO concentration was measured as explained in the methods section. As we can see in the Figure S2, there is no difference between conditions.

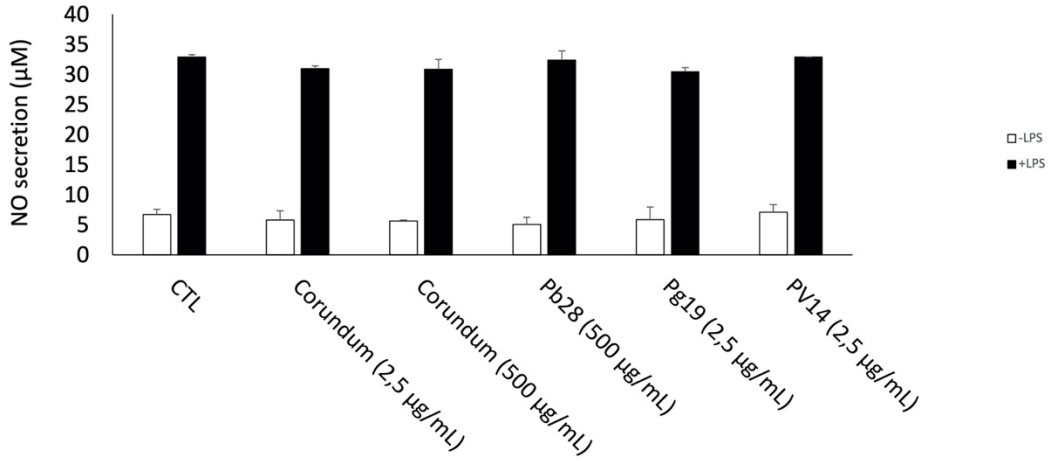
NO secretion (µM)
40
35
30
25
20
15
10
5
0
CTL
Corundum (2,5 µg/mL)
Corundum (500 µg/mL)
Pb28 (500 µg/mL)
Pg19 (2,5 µg/mL)
PV14 (2,5 µg/mL)
-LPS
+LPS